

A Sparse Graph-Structured Lasso Mixed Model for Genetic Association with Confounding Correction

Wenting Ye*, Xiang Liu†, Haohan Wang‡ and Eric P. Xing‡,§

Abstract

While linear mixed model (LMM) has shown a competitive performance in correcting spurious associations raised by population stratification, family structures, and cryptic relatedness, more challenges are still to be addressed regarding the complex structure of genotypic and phenotypic data. For example, geneticists have discovered that some clusters of phenotypes are more co-expressed than others. Hence, a joint analysis that can utilize such relatedness information in a heterogeneous data set is crucial for genetic modeling.

We proposed the sparse graph-structured linear mixed model (sGLMM) that can incorporate the relatedness information from traits in a dataset with confounding correction. Our method is capable of uncovering the genetic associations of a large number of phenotypes together while considering the relatedness of these phenotypes. Through extensive simulation experiments, we show that the proposed model outperforms other existing approaches and can model correlation from both population structure and shared signals. Further, we validate the effectiveness of sGLMM in the real-world genomic dataset on two different species from plants and humans. In *Arabidopsis thaliana* data, sGLMM behaves better than all other baseline models for 63.4% traits. We also discuss the potential causal genetic variation of Human Alzheimer’s disease discovered by our model and justify some of the most important genetic loci.

*School of Computer Science, Beijing University of Posts and Telecommunications, Beijing, 100876, China

†School of Information and Communication Engineering, Beijing University of Posts and Telecommunications, Beijing, 100876, China

‡School of Computer Science, Carnegie Mellon University, Pittsburgh, PA 15213, USA.

§Corresponding author. Email: epxing@cs.cmu.edu

1 Introduction

The recent years have witnessed a substantial advance in the exploration of the genetic architecture and linkage mapping between genetic markers and phenotypes. The advance of genome-wide association studies (GWAS) has helped scientists to discover genetic variants that are potentially causal to complex diseases [1, 2], such as the evaluation of human diseases like type 2 diabetes [3], comprehending evolutionary patterns [4] and assisting animal breeding programs [5].

However, identifying the genetic variants is still a challenging task. The most important feature of GWAS is their sheer scale. Hundreds of thousands of SNPs (single nucleotide polymorphisms) are now being typed on samples involving thousands of individuals. With the number of predictors far exceeding the number of observation, it's nearly impossible to employ the classical multivariate regression. Hence geneticists have to opt for simple univariate linear regression that analyzes one SNP at a time [6]. Given that most of the complex traits are polygenic, this apparently amounts to the model misspecification, resulting in false discovery whenever a lack of independence between loci (such as population structure) occurs [7, 8, 9].

Since the traditional methods are not expected to explain most of the genetic variations [10], biologists have developed many approaches to analyze polygenic effects [11, 12, 13]. The most popular method is ℓ_1 -norm regularization (i.e. lasso regression) [14]. Recent studies have extended the model capability by adding different regularizers [15], such as the smoothly clipped absolute deviation (SCAD) [16] and the minimax concave penalty (MCP) [17], which improve the performance by introducing non-smooth penalty in the optimization problem. However, the above-mentioned methods ignore the prolific dependency information between responses. Chen *et al* proposed graph-structured regression method (GFlasso) that can incorporate such information through a given correlation graph [18].

On the other hand, confounders like population structure will induce the spurious associations between the genotypes and phenotypes, caused by the deviation from the idealized i.i.d. assumption in statistics. Consequently, naïvely applying classic linear regression will lead to a substantial amount of false positive discoveries [19]. Two popular approaches to address this is principal components analysis (PCA) [20, 21] and linear mixed models [9, 22]. There is an increasing number of models proposed based on LMM due to the improvements that allow their application to human-scale genome data [23, 24]. The FaST-LMM-Select improves its performance by selecting a small number of SNPs systematically [25]. The BOLT-LMM requires fewer iterations and increases power by modeling more realistic, non-infinitesimal genetic architectures [26]. The liability-threshold mixed linear model overcomes the LMM's limitation in case-control ascertainment [27].

There have been several attempts to employ confounding correction and linkage mapping jointly [15, 28, 29]. Segura *et al* have proposed a related multi-locus mixed model using step-wise forward selection [30]. In parallel to our work, Rakitsch *et al* introduced a model called lasso multi-marker mixed model (sLMM) to solve this problem but only considering one single trait [31]. Korte *et al* extended the ability of LMM to carry out GWAS on correlated phenotypes. However, the proposed approach requires setting parameters for each pair of traits, and hence cannot scale to the large dataset [32].

In this article, we extend the recent solutions of sparse linear mixed model that can correct confounding factors and perform genetic association simultaneously further to account the relatedness between different traits. We propose a new-fashioned analysis method, named sparse graph-structured linear mixed model (sGLMM), that can reconstruct the convoluted phenotypic architecture in a dataset originated from different populations. The proposed model requires no

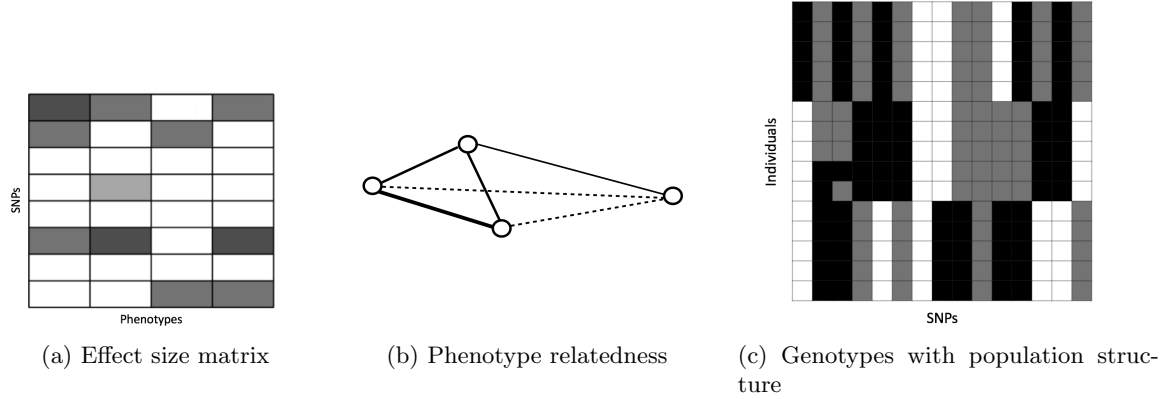


Figure 1: **An illustration of phenotypes relatedness and population structure as a confounding factor.** (a): The sparse and correlated phenotypic structure with white entries for zeros and gray entries for nonzero values. (b): The phenotypes relatedness graph corresponding to panel (a) with solid line for strong correlation and dotted line for weak correlation. It's clear that the three of the phenotypes have the strong connection between each other. (c): The dataset with population structure. The samples are originated from three populations and individuals from the same population tend to share common SNPs.

prior knowledge of the individual relationship and is capable of learning the structured pattern in a way that is properly calibrated to the degrees of traits' relatedness.

The rest of the paper is organized as follow. In Section 2, we introduce a novel method to accomplish both structured genetic association and confounding correction simultaneously. In Section 3, through extensive simulation experiments, we show the superiority of the proposed model in finding active SNPs. Then in Section 4 sGLMM is validated in the real-world genomic dataset from two different species and the discovered knowledge is discussed.

2 Model

In this section, the framework of the sparse linear mixed model will be introduced first. Then we propose the sparse graph-structured linear mixed model to extend sLMM by taking the relatedness between traits into consideration.

2.1 Sparse linear mixed model

Assume that data are collected for j SNPs and k phenotypes over n individuals. Let a $n \times j$ matrix \mathbf{X} denote the covariates, genotypes of each individual, and a $n \times k$ matrix \mathbf{y} stand for responses, traits of each individual. For each phenotype, we assume a standard liner mixed model as Equation 1:

$$\mathbf{y}_i = \mathbf{X}\boldsymbol{\beta}_i + \mathbf{u}_i + \boldsymbol{\epsilon}_i \quad (1)$$

where $\boldsymbol{\beta}_i$ is a $j \times 1$ vector for i -th trait's fixed effect, \mathbf{u}_i for random effect and $\boldsymbol{\epsilon}_i$ for observation noise. Both \mathbf{u}_i and $\boldsymbol{\epsilon}_i$ are $n \times 1$ vectors. Throughout this paper, we use subscripts to denote

columns and superscripts to denote rows, for example β_i and β^i are the i -th column and i -th row of β respectively, and β stands for the whole effect size matrix.

\mathbf{u}_i and ϵ_i are random variables with zero means, while having different covariances. The \mathbf{u}_i cannot be observed in a straight way, nonetheless, there are many avenues to obtain its covariance matrix \mathbf{K} . One is to employ the realized relationship matrix (RRM), a measure of genetic similarity to get the probabilities that pairs of individuals have causative alleles in common [13, 33, 34]. Marginalizing over the random effect \mathbf{u}_i will lead to a Gaussian marginal likelihood model [35]. Assuming that \mathbf{u}_i and ϵ_i follow the Gaussian distribution with covariance $\sigma_g^2 \mathbf{K}$ and $\sigma_\epsilon^2 \mathbf{I}$ respectively, we can conclude that:

$$\mathbf{y}_i \sim \mathcal{N}(\mathbf{X}\beta_i, \sigma_g^2 \mathbf{K} + \sigma_\epsilon^2 \mathbf{I}) \quad (2)$$

Assuming the priori distribution of β could be expressed as $e^{-\Phi(\beta)}$, we can define the likelihood function of the linear mixed model as:

$$\ell(\sigma_g^2, \sigma_\epsilon^2, \beta) = e^{-\Phi(\beta)} \cdot \prod_{i=1}^k \mathcal{N}(\mathbf{y}_i | \mathbf{X}\beta_i, \sigma_g^2 \mathbf{K} + \sigma_\epsilon^2 \mathbf{I}) \quad (3)$$

To accord with the reality that the majority of SNP's effect size are zero, sLMM assumes that β follows Laplace shrinkage prior, and the resulting $\Phi(\beta)$ could be written as Equation 4:

$$\Phi(\beta) = \lambda \|\beta\|_1 \quad (4)$$

Where $\|\cdot\|_1$ denotes the entry-wise matrix ℓ_1 -norm and λ controls the overall sparsity. As increasing λ , the fewer active genetic variants will be yielded. Substitute this penalty into Equation 3, we can get the sparse linear mixed model. However, this lasso penalty fails to consider the relatedness between different traits. Such defect drives us to the sparse graph-structured linear mixed model.

2.2 Sparse graph-structured linear mixed model

Based on the framework in Equation 3, we introduce the graph-fusion penalty to model the dependency between different traits. Given a graph G with a set of nodes $V = \{1, \dots, k\}$ and weighted edges E . The weight of the edge determines the degree of correlation. Here we construct such graph simply by computing pairwise Pearson correlation, and linking two nodes if their correlation is above a given threshold ρ . Let r_{ml} denotes the weight of edge $e = (m, l) \in E$ which measures the correlation between traits. Based on this graph, we can define $\Phi(\beta)$ as Equation 5:

$$\Phi(\beta) = \lambda \|\beta\|_1 + \gamma \sum_{e=(m,l) \in E} |r_{ml}| \sum_{i=1}^j |\beta_m^i - \text{sign}(r_{ml}) \beta_l^i| \quad (5)$$

Where λ controls the sparsity and γ controls the complexity of the model. Increasing the value of γ will make the correlated traits more likely to share a common set of causal SNPs. Substituting it into Equation 3, we can get the optimization equation for the proposed sGLMM.

2.3 Parameter Inference

Optimizing the hyper-parameter $\Theta = \{\sigma_g^2, \sigma_\epsilon^2, \lambda, \gamma\}$ is a NP-hard problem. Following the algorithm described in Rakitsch *et al*, we tune σ_g^2 and σ_ϵ^2 first without SNP effect, then reduce the problem to a standard graph lasso regression problem. Such procedure has been widely used in the single-SNP mixed models and shown the similar performance compared with an exact manner [9].

2.3.1 Null model fitting

To begin with, we first optimize σ_g^2 and σ_ϵ^2 without the effect of β . Instead of tuning σ_g^2 and σ_ϵ^2 respectively, we optimize the ratio of them [23], $\delta = \sigma_\epsilon^2 / \sigma_g^2$:

$$\ell_{null}(\sigma_g, \delta) = e^{-\Phi(\beta)} \cdot \prod_{i=1}^k \mathcal{N}(\mathbf{y}_i | \mathbf{X}\beta_i, \sigma_g^2(\mathbf{K} + \delta\mathbf{I})) \quad (6)$$

In general, we first compute the spectral decomposition of $\mathbf{K} = \mathbf{U}\text{diag}(\mathbf{d})\mathbf{U}^T$, where \mathbf{U} for eigenvector matrix and $\text{diag}(\mathbf{d})$ for eigenvalue matrix. After that we reweigh the data to make the covariance of the Gaussian distribution isotropic. Then, we carry out a one-dimension optimization with regard to δ to optimize the log-likelihood, while σ_g can be optimized in closed form during each evaluation.

2.3.2 Reduction to standard graph-guided fused lasso

Having the resulting optimized δ and σ_g , we utilize the eigen decomposition of \mathbf{K} again to reweigh the data such that the covariance matrix becomes isotropic:

$$\begin{aligned} \tilde{\mathbf{X}} &= (\text{diag}(\mathbf{d}) + \delta\mathbf{I})^{-\frac{1}{2}}\mathbf{U}^T\mathbf{X} \\ \tilde{\mathbf{y}}_i &= (\text{diag}(\mathbf{d}) + \delta\mathbf{I})^{-\frac{1}{2}}\mathbf{U}^T\mathbf{y}_i \end{aligned}$$

Where $\tilde{\mathbf{y}}_i$ denotes the rescaled phenotypes and $\tilde{\mathbf{X}}$ for genotypes. After that, Equation 3 can be rewritten as Equation 7:

$$\ell_{reweighed}(\beta) = e^{-\Phi(\beta)} \cdot \prod_{i=1}^k \mathcal{N}(\tilde{\mathbf{y}}_i | \tilde{\mathbf{X}}\beta_i, \sigma_g^2\mathbf{I}) \quad (7)$$

After such transformation, the task is equivalent to the standard graph-structured regression model:

$$\hat{\beta} = \min_{\beta} \frac{1}{\sigma_g^2} \left\| \tilde{\mathbf{y}} - \tilde{\mathbf{X}}\beta \right\|_F^2 + \Phi(\beta) \quad (8)$$

Here, $\|\cdot\|_F$ denotes the matrix Frobenius norm, and Φ is determined by Equation 5. To solve this problem efficiently, we employ the smoothing proximal gradient descent method [36].

3 Simulation study

In this section, we evaluate the performance of the proposed sGLMM model against vanilla sparse linear mixed models as well as other classical variable selection methods.

3.1 Data generation

To get the appropriate dataset with the relatedness of genes and population structure, we break the generation into three steps: generation of 1) SNPs 2) effect size matrix and 3) phenotypes.

Generation of SNPs To begin with, we need to generate the SNPs originated from g different populations. We use c_i to symbolize the centroid of the i -th population, $i = 1, \dots, g$. First, we generate centroids of g different distributions, and then SNP data from a multivariate Gaussian distribution as follows:

$$x_i \sim \mathcal{N}(c_j, \sigma_s^2 I)$$

where x_i denotes the i -th individual originated from j -th distribution and σ_s^2 controls the magnitude of covariance of subpopulation. Decreasing σ_s will result in stronger population structure.

Generation of effect size matrix We generate the effect size matrix β_k such that the output traits are correlated in a block-like structure. The generated traits are divided into g_{num} clusters in the experiment, and each cluster shares a common set of relevant SNPs. Another set of active SNPs is added to the first two clusters, simulating the situation of a higher-level correlation structure. In the end, the rows and columns are reordered randomly. An illustrative example was generated and demonstrated in Figure S1.

Generation of phenotypes We then generate a $n \times k$ intermediate output r from \mathbf{X} using the usual linear regression model:

$$r = X\beta + \epsilon$$

Here β is the resulting sparse matrix indicating which SNP in \mathbf{X} influences the gene expression r and $\epsilon \sim \mathcal{N}(0, \sigma_e^2 I)$. Since the generated β is correlated, the block-like structure dependency will be passed to the r automatically.

After that, to simulate a scenario with confounding factors, we introduce a covariance matrix to simulate correlations between the traits:

$$t_i \sim \mathcal{N}(r_i, \sigma_t^2 M)$$

Where t is a $n \times k$ intermediate output and M is the covariance between traits caused by population structure and σ_t^2 is a scalar that controls the magnitude of covariance. Letting C be the matrix formed by stacking the centroid of each individual, we choose $M = CC^T$. This has the desired effect of making observations from the same population more correlated.

In the end, to simulate the correlation between traits caused by the shared signals, we introduce one more covariance between traits. Each row of final trait matrix can be expressed as:

$$\mathbf{y}^i \sim \mathcal{N}(t^i, \sigma_m^2 S)$$

Where S measures the covariance between traits caused by shared signals and σ_m^2 is a scalar that controls the magnitude. Here we let $S = \beta^T \beta$, which has the desired effect of making dependent traits to be more correlated.

Table 1: Default parameter setting in the simulation study

Parameter	Default	Description
n	1000	the number of samples
j	5000	the number of SNPs
k	50	the number of traits
d	10%	the percentage of active SNPs
g	5	the number of subpopulations
g_{num}	3	the number of correlated trait clusters
σ_s^2	0.005	the magnitude of covariance of subpopulations
σ_t^2	100	the magnitude of covariance of traits caused by genetic effect
σ_m^2	0.001	the magnitude of covariance of traits caused by shared signals
σ_e^2	50	the magnitude of covariance of noise

3.2 Experimental results

The default parameters we used in our simulations are listed in Table 1. We adjust each of these 10 parameters to evaluate the performance of our model under different circumstances. We tested the proposed model as well as the following models:

- lasso, the most classical regression method used in variable selection [14].
- SCAD (smoothly clipped absolute deviation), a method which provides continuity, sparsity, and unbiasedness by using a symmetric, nonconcave penalty[16].
- GFlasso (graph-guided fused lasso), a multi-task regression method that incorporates the dependency information as a graph [18].
- FaST-LMM-Select, an approach which considers a small number of SNPs systematically to improve its performance [25].
- BOLT, a model which utilizes more realistic, non-infinitesimal genetic architectures to reduce the needed iteration and increase linkage power [26].
- sLMM (sparse linear mixed model), a mixed model that allows for both multi-locus mapping and correction for confounding effect [31].
- MCP (minimax concave penalty), a method that provides fast, continuous, nearly unbiased and accurate variable selection [37].

The results are shown as receiver operating characteristic (ROC) curves¹ in Figure 2. Due to the limitation of space, here we only show the low false positive rate (FPR) part of ROC curves in some experimental settings. The full ROC curves for all experimental settings are in Figure

¹The problem can be regarded as classification problem–identifying the active genetic variants from all genes. So for each threshold, we select the genetic variants whose absolute effect sizes are higher than the threshold. If the selected SNP has non-zero value in ground truth effect size, it will be a true positive of this problem.

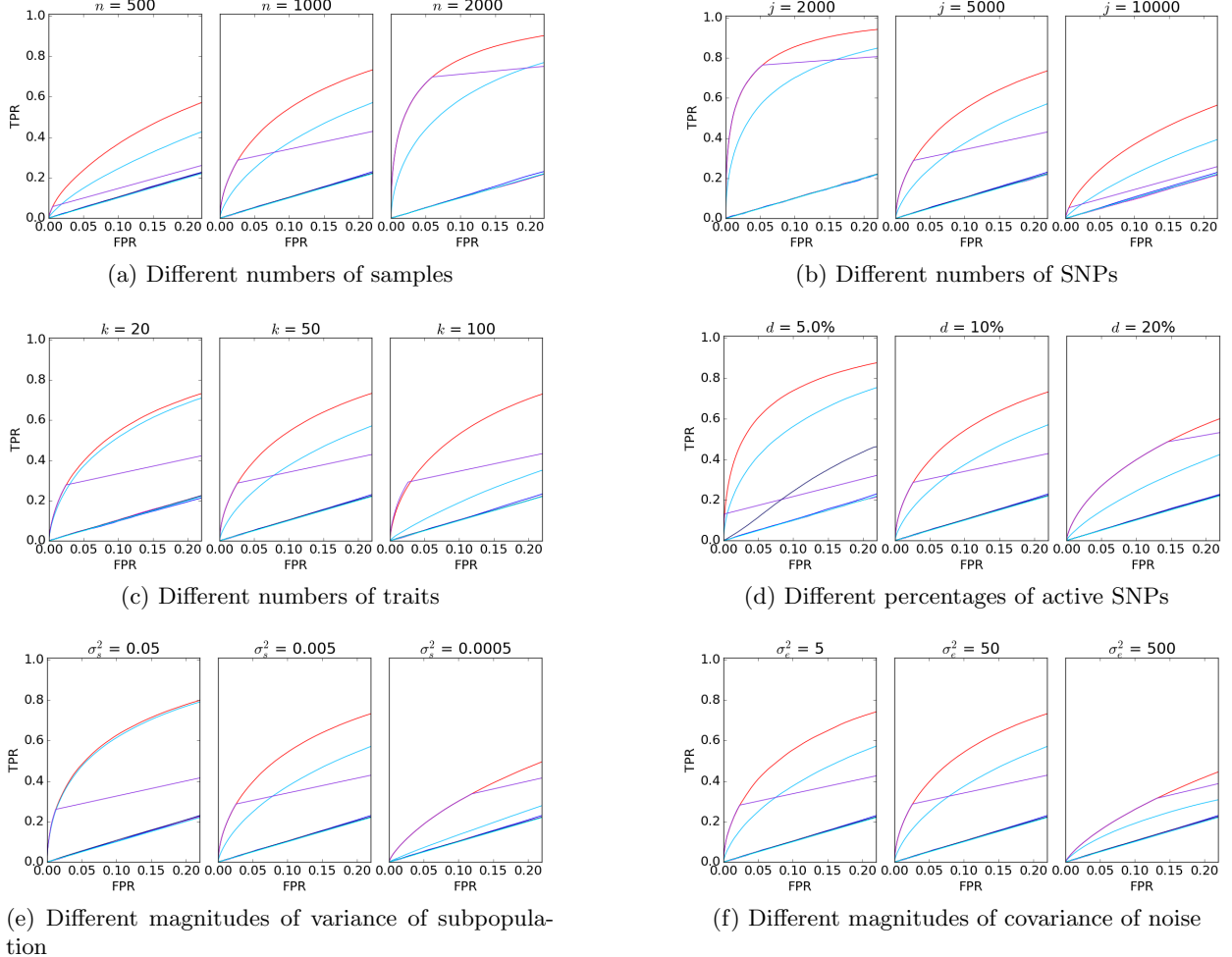


Figure 2: **Receiver operating characteristic (ROC) curves for experiments with various parameters.** We show low FPR part of ROC curves to compare our method with existing methods. For each configuration, the reported curve is drawn over ten random seeds.

S3. The precision-recall curves are displayed in Figure S4. For each setting tested, we generated different data by ten random seeds and then drew the overall results. We also prove sGLMM’s ability to reconstruct the traits relatedness is better than GFlasso in Figure S2.

In general, the proposed sGLMM model behaves better than the other approaches in all parameter settings. FaST-LMM-Select, sLMM and GFlasso can extract some meaningful information while other traditional methods could barely find correct genetic variation throughout the whole experiment. The failure of these models proves the importance of modeling multi-source correlation in the data. As the percentage of active SNPs decreases in Figure 2d, the problem becomes less challenging, and all models behave better in a certain degree (it is the only setting where FaST-LMM-Select works), while sGLMM can keep efficient even when the training set is extremely

deficient (5000 SNPs with only 500 samples). Moreover, as illustrated in Figure 2c and Figure S3f, sGLMM shows its capability of handling traits relatedness pattern in different settings. Manipulating magnitude of confounding and trait dependency as in Figure 2e, Figure S3h and Figure S3i, we notice that GFlasso and sLMM behave well only when they model the major source of correlation. For example, in Figure 2e where $\sigma_s^2 = 0.05$, GFlasso can behave as well as sGLMM, but when $\sigma_s^2 = 0.0005$, GFlasso is much worse than sGLMM due to population structure. By contrast, sGLMM can keep stable performance in all settings through modeling multi-source correlation automatically. Interestingly, sLMM’s ROC curve coincides in part with our proposed model, suggesting these two models attach the biggest effect size to the same set of SNPs. However, the sGLMM overshadows sLMM by capturing the weak association in the data through utilizing the relatedness information.

4 Real genome data experiment

Having shown the efficiency of sGLMM in simulated datasets, we now demonstrate the proposed model is also an effective method in real datasets. To evaluate the method, we identify genetic variants in Alzheimer’s disease (AD) and *Arabidopsis thaliana*, and then we evaluate our findings with the published results in relevant literature to show the reliability of our methods compared with existing approaches. The details of preprocessing the data are described in Appendix.

4.1 Data Sets

4.1.1 *Arabidopsis thaliana*

The *Arabidopsis thaliana* dataset we obtained is a collection of around 200 plants, each with around 215,000 genetic variables [38]. We identified the causal genetic variables of 44 observed traits such as days to germination, days to flowering, lesioning, etc. These plants were distributed from 27 different countries in Europe and Asia, resulting in a potential confounding factor. For instances, different geographic origins may have different moisture and air conditions, which could affect the observed traits of the plants. Besides there are some correlated traits such as FT10, FT16 and FT20, which measure the flowering time in different temperature.

4.1.2 Alzheimer’s disease

We use the late-onset Alzheimer’s disease data provided by Harvard Brain Tissue Resource Center and Merck Research Laboratories [39]. It consists of measurements of 540 patients with 500,000 genetic variables. We tested the association between these SNPs and 28 phenotypes corresponding to a patient’s disease status of Alzheimer’s disease.

4.2 *Arabidopsis thaliana*

Since we have access to a validated gold standard of *Arabidopsis thaliana* dataset, we could directly assess their performance by ROC curve, the same metric used in the simulation study.

Figure 3 illustrates the area under the ROC curve (auROC) according to different traits. Generally speaking, our approach proves itself well suited to the real-world genomic dataset and outperforms all other methods for 63.4% traits. The overall average auROC of proposed sGLMM is 0.96, while the other models’ are lower than 0.78. Since there should be some traits not suffering

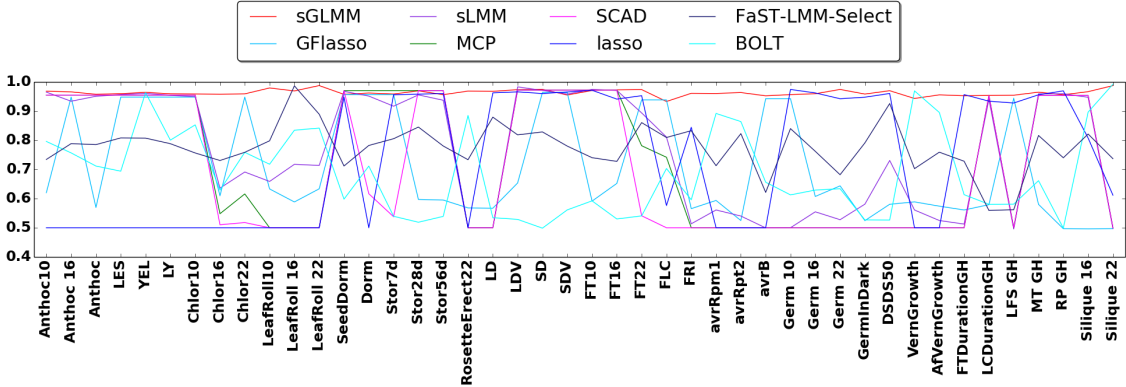


Figure 3: **Area under ROC curve for the 44 traits of *Arabidopsis thaliana*.**

from the confounders, it is barely surprising that the traditional methods (e.g., MCP, GFlasso, SCAD) behave well in this case. For example, the phenotypes beginning with “FT” like FT10 measure the average flowering time of days and the following numbers denote the environmental temperature. In these case, the time of daylight and temperature are rigorously controlled. As a result, the confounding introduced by the geographic origin is weakened.

4.3 Alzheimer’s disease

We list the ten most significant SNPs among all phenotypes found by our model in table 2 and validate their potential association with Alzheimer’s disease with previous research report.

To evaluate the accuracy of our model, here we justify SNPs discovered by our model. The 1st discovered SNP is corresponded to *C4orf50* gene, which can influence tissue-restricted expression level for the brain [40]. Both the 2nd and 4th are associated with *MACROD2* gene. *MACROD2* is expressed in the brain and associated with disorders such as autism [41], which is also reported to be associated with Alzheimer’s disease by other model [42]. The 5th and 6th are expressed by the *TENM1* gene, which codes the Teneurin Transmembrane Protein. This protein helps to build appropriate patterns of neural connectivity, playing a crucial role in visual, olfactory and motor systems [43, 44]. The 8th SNP is associated with *CD70* gene, which is surface molecules expressed by Mature T-cells [45, 46]. Biologists have found that the level of T-cells in AD brain is much higher than in unaffected patients [47, 48]. With six of the reported SNPs are associated with brain or directly with Alzheimer’s disease, the estimated false positive rate is 40%.

5 Discussion

The computational complexity of the two-stage algorithm mainly depends on the optimization of GFlasso regression. The difference between our method and graph-guided fused lasso regression is $O(n^3)$ for decomposition of \mathbf{K} , $O(n^2j+njk)$ for reweighing the phenotype matrix \mathbf{y} and genotypes \mathbf{X} (computing $\mathbf{U}^T\mathbf{y}$ and $\mathbf{U}^T\mathbf{X}$), and $O(njk)$ for execution of the log likelihood in the one-dimensional optimization over δ for constant times.

Our model has been implemented in Python and is free available². Currently, it supports both

²<https://github.com/YeWenting/sGLMM>

Table 2: Discovered SNPs related to Alzheimer’s disease

Rank	SNP	Chr	Chr Position	RefSNP Alleles	MAF	Gene
1	rs9999966	4	5925628	C/T	0.0807	C4orf50
2	rs16994889	20	14746661	A/G	0.0791	MACROD2
3	rs1699451	7	69288571	A/G	0.3908	
4	rs16994542	20	14409645	A/C	0.2764	MACROD2
5	rs16994557	X	125041417	C/T	0.2238	TENM1
6	rs16994560	X	125047265	C/T	0.0816	TENM1
7	rs16994583	X	148473389	A/G	0.0321	
8	rs16994592	19	6586487	C/T	0.0775	CD70
9	rs16994602	4	38536223	A/C/G	0.1492	
10	rs1699463	9	23853359	A/G	0.4139	

csv and plink format files. You can either specify the hyper-parameters or provide the program with the number of selected SNPs, otherwise the program will execute the cross validation. The detailed instruction is described in the Appendix.

In this paper, we apply a simple strategy to construct dependency graph G . However, sGLMM itself does not specify how G is obtained, so other more sophisticated approaches may be used.

6 Conclusion

In this article, we address the challenging problem in genome-wide association studies, exploring the genetic association where the data is non-i.i.d. and traits involve complex relatedness. There have been a wealth of attempts to utilize the advantages of LMM while losing sight of the interdependency among the traits. The method like graph-guided fused lasso enables the analysts to learn SNPs with pleiotropic effects that influence the activities of multiple co-expressed genes.

To solve this problem, we proposed the sparse graph-structured linear mixed model for genetic association. Our method not only corrects the irrelevant confounding but also utilizes the information of the relatedness of phenotypes into statistical analysis. We have shown that the traditional graph lasso can easily fall into the trap of utilizing false dependency information due to the confounding and using linear mixed model alone fails to capture the complex phenotypic architecture. In comparison to these approaches, sGLMM combines the advantages of both methods and remains computationally efficient. Through extensive experiments on both synthetic and real datasets, we exhibit sGLMM has a clear superiority over existing methods.

Funding

This material is based upon work funded and supported by the Department of Defense under Contract No. FA8721-05-C-0003 with Carnegie Mellon University for the operation of the Software Engineering Institute, a federally funded research and development center. This work is also supported by the National Institutes of Health grants R01-GM093156 and P30-DA035778.

References

- [1] Kim, B., Shah, J. A. & Doshi-Velez, F. Mind the gap: A generative approach to interpretable feature selection and extraction. In *Advances in Neural Information Processing Systems*, 2260–2268 (2015).
- [2] Wang, J., Fujimaki, R. & Motohashi, Y. Trading interpretability for accuracy: Oblique treed sparse additive models. In *Proceedings of the 21th ACM SIGKDD International Conference on Knowledge Discovery and Data Mining*, 1245–1254 (ACM, 2015).
- [3] Craddock, N. *et al.* Genome-wide association study of cnvs in 16,000 cases of eight common diseases and 3,000 shared controls. *Nature* **464**, 713–720 (2010).
- [4] Kruuk, L. E. Estimating genetic parameters in natural populations using the animal model. *Philosophical Transactions of the Royal Society of London B: Biological Sciences* **359**, 873–890 (2004).
- [5] Meyer, K., Johnston, D. J. & Graser, H.-U. Estimates of the complete genetic covariance matrix for traits in multi-trait genetic evaluation of australian hereford cattle. *Crop and Pasture Science* **55**, 195–210 (2004).
- [6] McCarthy, M. I. *et al.* Genome-wide association studies for complex traits: consensus, uncertainty and challenges. *Nature reviews genetics* **9**, 356–369 (2008).
- [7] Hoggart, C. J., Whittaker, J. C., De Iorio, M. & Balding, D. J. Simultaneous analysis of all snps in genome-wide and re-sequencing association studies. *PLoS Genet* **4**, e1000130 (2008).
- [8] Price, A. L., Zaitlen, N. A., Reich, D. & Patterson, N. New approaches to population stratification in genome-wide association studies. *Nature Reviews Genetics* **11**, 459–463 (2010).
- [9] Kang, H. M. *et al.* Variance component model to account for sample structure in genome-wide association studies. *Nature genetics* **42**, 348–354 (2010).
- [10] Visscher, P. M., Brown, M. A., McCarthy, M. I. & Yang, J. Five years of gwas discovery. *The American Journal of Human Genetics* **90**, 7–24 (2012).
- [11] Wu, T. T., Chen, Y. F., Hastie, T., Sobel, E. & Lange, K. Genome-wide association analysis by lasso penalized logistic regression. *Bioinformatics* **25**, 714–721 (2009).
- [12] Logsdon, B. A., Hoffman, G. E. & Mezey, J. G. A variational bayes algorithm for fast and accurate multiple locus genome-wide association analysis. *BMC bioinformatics* **11**, 58 (2010).
- [13] Yang, J. *et al.* Common snps explain a large proportion of the heritability for human height. *Nature genetics* **42**, 565–569 (2010).
- [14] Tibshirani, R. Regression shrinkage and selection via the lasso. *Journal of the Royal Statistical Society. Series B (Methodological)* 267–288 (1996).
- [15] Fan, Y. & Li, R. Variable selection in linear mixed effects models. *Annals of statistics* **40**, 2043 (2012).

- [16] Fan, J. & Li, R. Variable selection via nonconcave penalized likelihood and its oracle properties. *Journal of the American statistical Association* **96**, 1348–1360 (2001).
- [17] Zhang, C.-H. *et al.* Nearly unbiased variable selection under minimax concave penalty. *The Annals of statistics* **38**, 894–942 (2010).
- [18] Chen, X., Kim, S., Lin, Q., Carbonell, J. G. & Xing, E. P. Graph-structured multi-task regression and an efficient optimization method for general fused lasso. *arXiv preprint arXiv:1005.3579* (2010).
- [19] Astle, W. & Balding, D. J. Population structure and cryptic relatedness in genetic association studies. *Statistical Science* 451–471 (2009).
- [20] Price, A. L. *et al.* Principal components analysis corrects for stratification in genome-wide association studies. *Nature genetics* **38**, 904–909 (2006).
- [21] Patterson, N., Price, A. L. & Reich, D. Population structure and eigenanalysis. *PLoS genet* **2**, e190 (2006).
- [22] Goddard, M. Genomic selection: prediction of accuracy and maximisation of long term response. *Genetica* **136**, 245–257 (2009).
- [23] Lippert, C. *et al.* Fast linear mixed models for genome-wide association studies. *Nature methods* **8**, 833–835 (2011).
- [24] Pirinen, M., Donnelly, P., Spencer, C. C. *et al.* Efficient computation with a linear mixed model on large-scale data sets with applications to genetic studies. *The Annals of Applied Statistics* **7**, 369–390 (2013).
- [25] Listgarten, J. *et al.* Improved linear mixed models for genome-wide association studies. *Nature methods* **9**, 525–526 (2012).
- [26] Loh, P.-R. *et al.* Efficient bayesian mixed-model analysis increases association power in large cohorts. *Nature genetics* **47**, 284–290 (2015).
- [27] Hayeck, T. J. *et al.* Mixed model with correction for case-control ascertainment increases association power. *The American Journal of Human Genetics* **96**, 720–730 (2015).
- [28] Bondell, H. D., Krishna, A. & Ghosh, S. K. Joint variable selection for fixed and random effects in linear mixed-effects models. *Biometrics* **66**, 1069–1077 (2010).
- [29] Wang, H. & Yang, J. Multiple confounders correction with regularized linear mixed effect models, with application in biological processes. *bioRxiv* 089052 (2016).
- [30] Segura, V. *et al.* An efficient multi-locus mixed-model approach for genome-wide association studies in structured populations. *Nature genetics* **44**, 825–830 (2012).
- [31] Rakitsch, B., Lippert, C., Stegle, O. & Borgwardt, K. A lasso multi-marker mixed model for association mapping with population structure correction. *Bioinformatics* **29**, 206–214 (2013).
- [32] Korte, A. *et al.* A mixed-model approach for genome-wide association studies of correlated traits in structured populations. *Nature genetics* **44**, 1066–1071 (2012).

- [33] Goddard, M. E., Wray, N. R., Verbyla, K., Visscher, P. M. *et al.* Estimating effects and making predictions from genome-wide marker data. *Statistical Science* **24**, 517–529 (2009).
- [34] Hayes, B. J., Visscher, P. M. & Goddard, M. E. Increased accuracy of artificial selection by using the realized relationship matrix. *Genetics research* **91**, 47–60 (2009).
- [35] Kang, H. M. *et al.* Efficient control of population structure in model organism association mapping. *Genetics* **178**, 1709–1723 (2008).
- [36] Chen, X., Lin, Q., Kim, S., Carbonell, J. G. & Xing, E. P. Smoothing proximal gradient method for general structured sparse regression. *The Annals of Applied Statistics* 719–752 (2012).
- [37] Zhang, Z. *et al.* Mixed linear model approach adapted for genome-wide association studies. *Nature genetics* **42**, 355–360 (2010).
- [38] Anastasio, A. E. *et al.* Source verification of mis-identified arabidopsis thaliana accessions. *The Plant Journal* **67**, 554–566 (2011).
- [39] Zhang, B. *et al.* Integrated systems approach identifies genetic nodes and networks in late-onset alzheimers disease. *Cell* **153**, 707–720 (2013).
- [40] Delgado, A., Brandao, P. & Narayanan, R. Diabetes associated genes from the dark matter of the human proteome. *MOJ Proteomics Bioinform* **1**, 00020 (2014).
- [41] Anney, R. *et al.* A genome-wide scan for common alleles affecting risk for autism. *Human molecular genetics* **19**, 4072–4082 (2010).
- [42] Kohannim, O. *et al.* Discovery and replication of gene influences on brain structure using lasso regression. *Frontiers in neuroscience* **6** (2012).
- [43] Leamey, C. A. & Sawatari, A. The teneurins: new players in the generation of visual topography. In *Seminars in cell & developmental biology*, vol. 35, 173–179 (Elsevier, 2014).
- [44] Alkelai, A. *et al.* A role for tenm1 mutations in congenital general anosmia. *Clinical genetics* **90**, 211–219 (2016).
- [45] Romero, P. *et al.* Four functionally distinct populations of human effector-memory cd8+ t lymphocytes. *The Journal of Immunology* **178**, 4112–4119 (2007).
- [46] Salaun, B. *et al.* Differentiation associated regulation of microrna expression in vivo in human cd8+ t cell subsets. *Journal of translational medicine* **9**, 44 (2011).
- [47] Sardi, F. *et al.* Alzheimer’s disease, autoimmunity and inflammation. the good, the bad and the ugly. *Autoimmunity reviews* **11**, 149–153 (2011).
- [48] Song, J. & Lee, J. E. mir-155 is involved in alzheimers disease by regulating t lymphocyte function. *Frontiers in aging neuroscience* **7** (2015).

Appendix

Instructions of using the software sGLMM

Our codes are available on line and anyone can follow the installation instruction at <https://github.com/YeWenting/sGLMM> and can also use sGLMM as a stand alone script without installation.

Run

```
python runsGLMM.py -help
```

to see available options as following:

Table S1: The options of the sGLMM's program

Parameter	Description
-h, --help	show help message
-t FILETYPE	choices of input file type (only csv or plink)
-n FILENAME	name of the input file
-lambda=LMBD	the weight of the penalizer. If neither lambda nor snum is given, cross validation will be run.
-snum=SNUM	the number of targeted variables the model selects for each trait. If neither lambda nor snum is given, cross validation will be run.
-threshold=TH	the threshold to mask the weak phenotype relatedness
-q	run in a quiet mode
-m	run without missing genotype imputation

Specify selected SNP number:

```
python runsGLMM.py -snum=50 -n data/mice.plink
```

This command will train the sGLMM repeatedly until the number of non-zero effect sizes for each trait is close to 50. The selected SNPs will be stored in data/mice.plink.output.

Specify λ :

```
python runsGLMM.py -lambda=2 -n data/mice.plink
```

This command will set the hyper-parameter λ to 2, and then train the sGLMM under such setting. The selected SNPs will be stored in data/mice.plink.output.

Naïve Usage:

```
python runsGLMM.py -n data/mice.plink
```

This command does not require the user to specify any arguments. The sGLMM will perform cross validation to select the appropriate regularization weight. The selected SNPs will be stored in data/mice.plink.output.

Simulation study

Demo effect size matrix in simulation study

The Figure S1 shows a demo effect size matrix generated in the simulation study ³. For illustration, we make more active SNPs than in the simulation experiment. From the picture, we could find that

³Where $j = 30$, $k = 10$ and $g_num = 3$ were used.

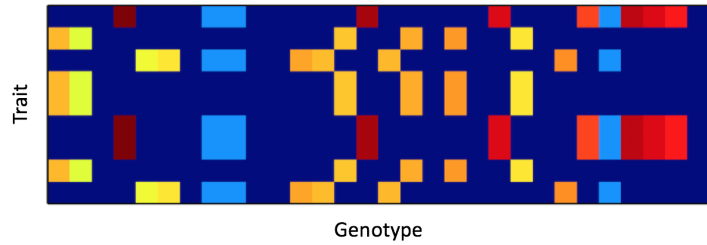


Figure S1: **Generation of effect size matrix.**

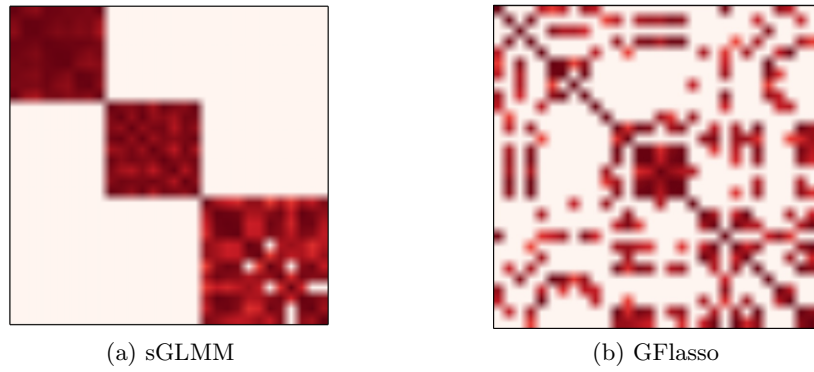


Figure S2: **Recovery of trait relatedness matrix**, where threshold $\rho = 0.618$ and other parameters are set as default. For illustration, the phenotypes here have not been reordered randomly. The red block implies the strong relatedness between traits while the white means week relation.
 (a) sGLMM (b) GFllasso

each cluster shares a common set of relevant loci with the similar strength. Further, a higher-level correlation structure across two subgraphs is colored with cerulean in this example.

Recovery of traits relatedness

Here we examine the capability of sGLMM to reconstruct the underlying relatedness among traits in Figure S2. Given that the whole phenotypes could be divided into three groups, the existence of population structure increases the difficulty in reconstructing the dependency between traits. However, Figure S2 reveals that sGLMM is still able to discover the block-like structure even under such confounder.

Full ROC curves in all experimental settings

The Figure S3 shows the full images of ROC curves in the simulation study to compare our method with other existing methods. For each configuration, the reported curve is drawn over ten random seeds.

The precision-recall curves of simulation study

The Figure S4 shows the full images of precision-recall curves in simulation study to compare our method with other existing methods. For each configuration, the reported curve is drawn over ten random seeds.

Preprocessing of real genomic data

Each element of the X takes values from $\{0,1,2\}$ according to the number of minor alleles at the given locus in each individual. We also standardized the traits data with zero mean and variance equals to 1 for each phenotype. The missing genotypes are imputed by filling in 0s since 0 is the most common genotype. The missing traits are imputed with filling in the statistical mean if it's a continuous trait, or mode if it's a categorical trait.

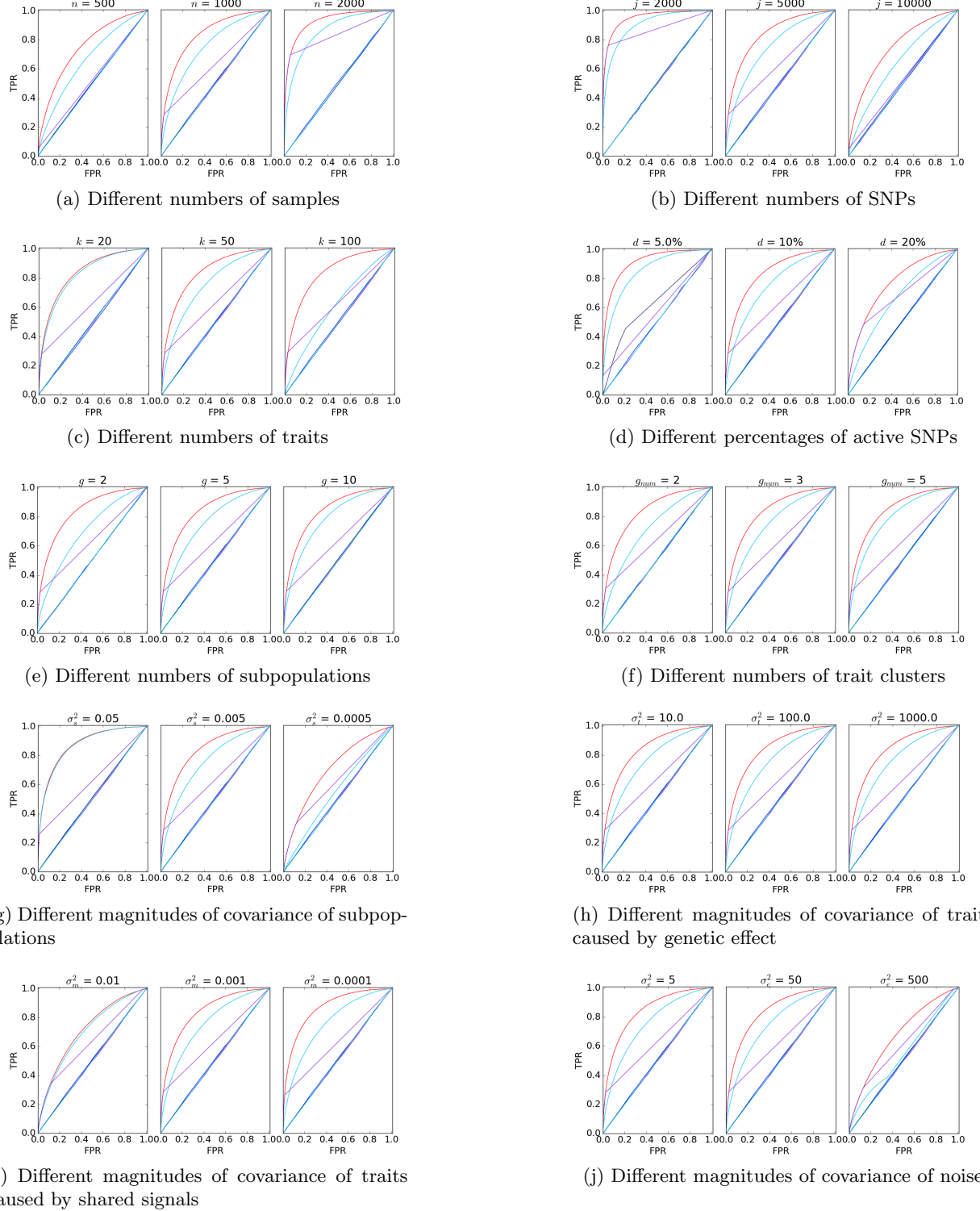


Figure S3: Full ROC curves for all experimental settings.

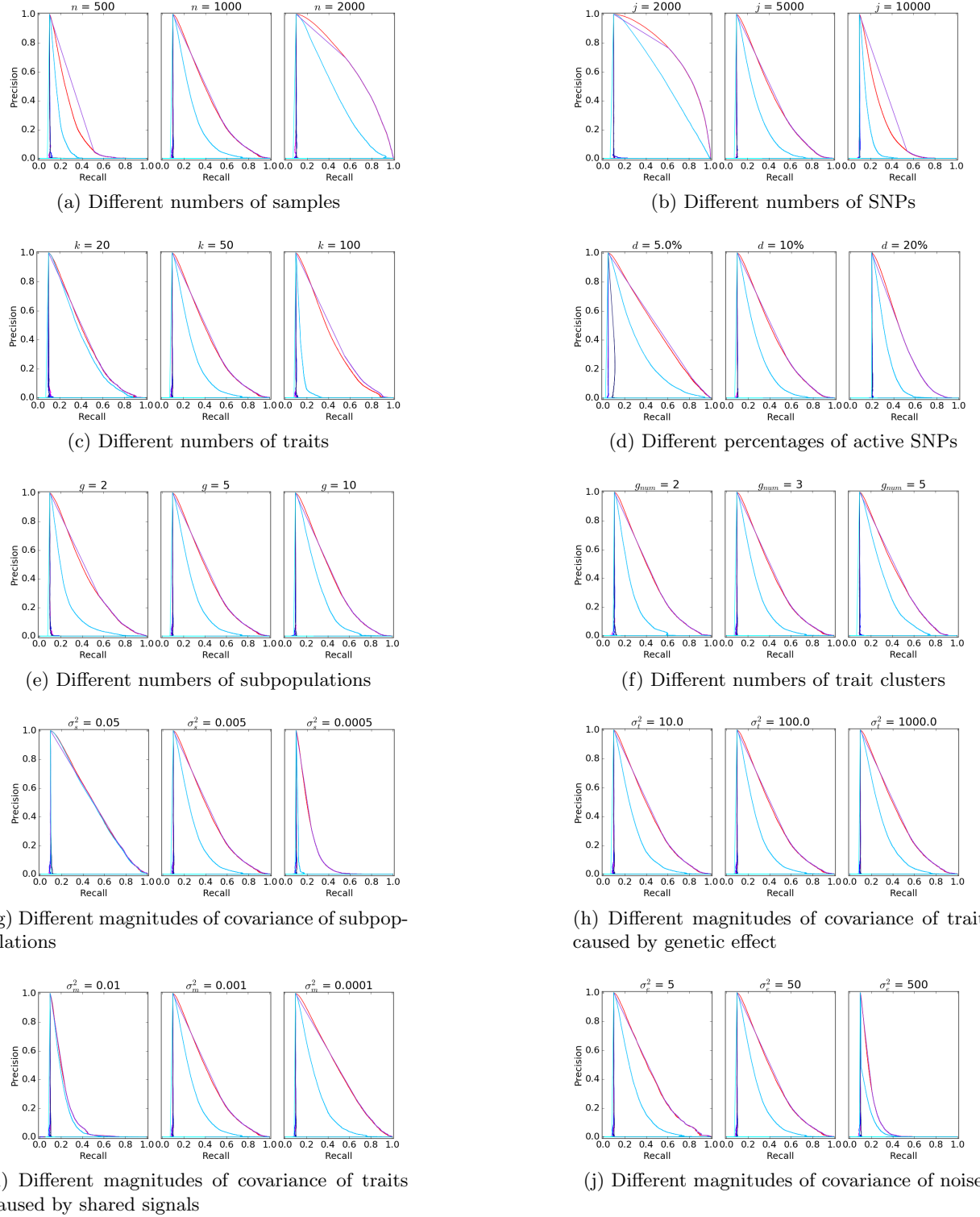


Figure S4: Precision-recall curves for experiment with different parameters.